Magdalena J. Ślusarz
Rafał Ślusarz
Jerzy Ciarkowski
Faculty of Chemistry,
University of Gdańsk,
Sobieskiego 18,
80-952 Gdańsk,
Poland

Investigation of Mechanism of Desmopressin Binding in Vasopressin V2 Receptor versus Vasopressin V1a and Oxytocin Receptors: Molecular Dynamics Simulation of the Agonist-Bound State in the Membrane–Aqueous System

Received 4 October 2005;
revised 21 November 2005;
accepted 21 November 2005
Published online 6 December 2005 in Wiley InterScience (www.interscience.wiley.com). DOI 10.1002/bip.20420

Abstract: *The vasopressin V2 receptor (V2R) belongs to the Class A G protein–coupled receptors (GPCRs). V2R is expressed in the renal collecting duct (CD), where it mediates the antidiuretic action of the neurohypophyseal hormone arginine vasopressin (CYFQNCPRG-NH_2, AVP). Desmopressin ([1-deamino, 8-D]AVP, dDAVP) is strong selective V2R agonist with negligible pressor and uterotonic activity. In this paper, the interactions responsible for binding of dDAVP to vasopressin V2 receptor versus vasopressin V1a and oxytocin receptors has been examined. Three-dimensional activated models of the receptors were constructed using the multiple sequence alignment and the complex of activated rhodopsin with Gt_α C-terminal peptide of transducin MII–Gt_α (338–350) prototype (Ślusarz, R.; Ciarkowski, J. Acta Biochim Pol 2004 51, 129–136) as a template. The 1-ns unconstrained molecular dynamics (MD) of receptor–dDAVP complexes immersed in the fully hydrated 1-palmitoyl-2-oleoyl-*sn*-glycero-3-phosphatidylcholine (POPC) membrane model was conducted in an Amber 7.0 force field. Highly conserved transmembrane residues have been proposed as being responsible for V2R activation and G protein coupling. Molecular mechanism of the dDAVP binding has been suggested. The internal water molecules involved in an intricate network of the hydrogen bonds inside the receptor cavity have been identified and their role in the stabilization of the agonist-bound state proposed.* © 2005 Wiley Periodicals, Inc. Biopolymers 81: 321–338, 2006

This article was originally published online as an accepted preprint. The "Published Online" date corresponds to the preprint version. You can request a copy of the preprint by emailing the Biopolymers editorial office at biopolymers@wiley.com

Keywords: *desmopressin; dDAVP; GPCR; internal water; MD; receptor activation; V2R*

INTRODUCTION

G protein–coupled receptors (GPCRs) are the membrane proteins that mediate actions of many extracellular regulatory molecules as diverse as peptides, biogenic amines, amino acids, glycoproteins, phospholipids, nucleosides, and Ca^{2+} ions as well as a range of exogenous ligands as odorants, tastants, pheromones,

Correspondence to: M. J. Ślusarz; e-mail: magda@chem.univ.gda.pl

Table I Biological Activities of AVP, OT, dAVP, DAVP, and dDAVP Toward Respective Receptors

	V2R	V1aR	OTR	Reference
AVP(IU/mg)	465	412	17	28
OT(IU/mg)	5	5	450	28
dAVP(IU/mg)	1745 ± 385	346 ± 13	—	114
DAVP(IU/mg)	253 ± 44	1.1 ± 0.04	—	114
dDAVP(IU/mg)	1200 ± 126	0.39 ± 0.2	—	31

and photons of light.[1] Moreover, they are very important pharmaceutical drug targets and identification of a GPCR activation mechanism is the major requisite of rational drug design.[2,3] The largest and best-studied Class A of GPCRs[4] includes, among others, rhodopsin (RD) and the neurohypophyseal hormone receptors, which are the subject of this work. The X-ray structure of the inactive (dark) form of bovine RD[5–8] is the only crystal structure of GPCR resolved to atomic resolution. It is an agreement that RD makes a good structural template for other Class A members.[3,9–13] Accordingly, it was used as a template for building neurohypophyseal hormone receptor models in our previous investigations.[14–16] The neurohypophyseal hormone receptor subgroup includes three vasopressin receptors (V1aR, V1bR, and V2R) and a unique oxytocin receptor (OTR).[17–19] The main function mediated via V2R expressed in the collecting duct (CD) of the kidney is the regulation of water reabsorption and concentration of the urine (antidiuretic effect).[20] Mutations in the V2R gene are responsible for the X-linked form of nephrogenic diabetes insipidus (NDI).[21] V1aR mainly controls increase of blood pressure, whereas the stimulation of adrenocorticotropin hormone secretion is mediated via V1bR (also known as V3R), which is not a subject of this work.[22,23] OTR is involved mainly in the control of labor and lactation in the mammals.[24,25] Moreover, neurohypophyseal hormone receptors play a role in many reproductive, behavioral, and social functions.[26] V1aR, V1bR, and OTR are functionally coupled to the Gq/11 protein that stimulates the activity of phospholipase C and cytosolic calcium mobilization, whereas V2R is coupled to the Gs protein that stimulates adenylyl cyclase.[17,18] The cellular response resulting from receptor activation is mainly determined via a type of a coupled G protein. The molecular mechanism determining the selectivity of receptor–G protein interaction is important for understanding the signal transduction pathway.

The neurohypophyseal hormone receptors, as typical GPCRs members, share a common membrane topology, thus being membrane-embedded proteins built of a single long polypeptide chain that traverses the membrane seven times and forms the transmembrane domain consisting of seven α-helices (TM) successively connected with extracellular (EL) and intracellular (IL) loops.[5,9,11] Receptor activation is induced when diffusable extracellular agonist docks to the receptor binding cavity and causes the switch of the receptor protein from an inactive state to an active conformation capable of interacting with a G protein.[27] The nonapeptide hormone arginine vasopressin (CYFQNCPRG-NH_2, AVP), also termed the antidiuretic hormone (ADH), is an endogenous agonist of the vasopressin receptors. The second neurohypophyseal hormone oxytocin ([I3,L8]AVP, OT) binds to the vasopressin receptors with low affinity, however, it is a natural agonist of OTR.[28] AVP is released into the blood for interaction with respective receptors under two main stimuli, i.e., the response to low urine osmolality and changes in blood volume and pressure.[29] Vasopressin also displays to a low degree typical OT activities: uterine contraction and milk ejection.[28]

Desmopressin ([1-deamino, 8-D]AVP, dDAVP), the main subject of this investigation, is strong selective V2R agonist with negligible pressor and uterotonic activity.[30,31] It is widely used for treatment of central diabetes insipidus and primary nocturnal enuresis.[32,33] dDAVP also increases levels of the coagulation factor VIII in mild hemophilia A and von Willebrand factor in von Willebrand disease.[34–36] In Table I the biological activities of the neurohypophyseal hormones and AVP analogues: dAVP (1-deamino-arginine vasopressin), DAVP (8-D-arginine vasopressin), and dDAVP are given. It is known that the deamination of the AVP molecule results in almost four times the enhanced affinity toward V2R (see Table I), probably due to a change of the molecule conformation.[37] The deamination does not change affinity toward V1aR, while this receptor is very sensitive to substitution at position 8, and the presence of D-Arg in this position results in the very low pressor activity (see

Table I). Thus, the high V2R/V1aR selectivity of dDAVP results from absence of some critical receptor–ligand interactions in V1aR. Consequently, it has been established that single-residue Asp103 located in the first extracellular loop (EL1) of V2R is responsible for the high affinity binding of the dDAVP.[38]

To clarify molecular mechanism of receptor–ligand interactions, experimental investigations are indispensable. However, they provide limited information about the dynamics of the docking and activation processes as well as about the role of environment (lipid or water molecules). Computer simulations make it possible to investigate many aspects of binding and activation processes in detail and they interplay with experiments either confirming experimental results or providing a new hypothesis for experimental verification. Unfortunately, available force fields are not advanced enough to simulate the receptor activation via docking agonist and subsequent molecular dynamics (MD) simulation in timescales typical for GPCR activation. The crystal structure of GPCR (RD) also represents the inactive state of the receptor[5–8] and its activation mechanism is still poorly recognized. However, it has been accepted that RD activation involves an outward move of the TM6, TM7, and TM2 cytosolic halves along with adjacent loop parts, away from the 7TM bundle with the simultaneous clockwise (viewing from the cytosol) TM6 rotation.[39,40] These conformational rearrangements eventually result in conversion from rhodopsin to *meta*-rhodopsin (Meta II, MII). It is also known that the C-terminal peptide Gt_{α}(340–350) stabilizes MII.[41–44] Accordingly, an atomic-resolution model of the MII monomer complexed with the Gt_{α}(338–350) fragment has been proposed;[45] subsequently, it was used as the template for construction of activated neurohypophyseal hormone receptor models and the interacting fragments of respective G proteins: Gs_{α}(382–394); (IIQRMHLRQYELL) for V2R and $Gq/11_{\alpha}$(347–359); (TILQLNLKEYNLV) for V1aR and OTR.[46] These models were applied successfully in our former investigations concerning the interactions with OT and AVP.[46,47] The same models are currently used in this work for analysis of receptor–dDAVP interactions.

METHODS

Parametrization

Nonstandard amino acid residues and other structure fragments were parameterized as recommended in the Amber 7.0 manual.[48] Specifically, the point atom charges were fitted by applying the Resp procedure[49] to the electrostatic potential calculated in the 6-31G* basis set using the program Gamess.[50]

Models

The three-dimensional model of dDAVP was built using the coordinates of pressinoic acid[51] and the Biopolymer module of the Sybyl package.[52] The three-residue C-terminal tail of dDAVP was added in the Amber 7.0 force field.[48] The lowest-energy conformation of dDAVP was obtained using energy minimization followed by the simulated annealing protocol in Amber.[53] Nonetheless, regardless of the ''seed conformation'' of the ligand, the AutoDock program,[54] subsequently used for docking dDAVP to receptors, employs a modified genetic algorithm[55] to explore the conformational states of a flexible ligand. Hence, the extensive conformational changes do occur during docking and any reasonable initial dDAVP structure is considered satisfactory at this point.[54,56]

The three-dimensional models of activated neurohypophyseal hormone receptors (V2R, V1aR, and OTR) and the α subunit C-terminal fragments of suitable G protein necessary to keep the receptor in an activated state were constructed as described previously,[46] using the model of MII–Gt_{α}(338–350), which is the appropriate modification of the x-ray RD structure,[5] as a template. Briefly, all computer modifications necessary to obtain neurohypophyseal receptor models were made using standard Amber 7.0 tools[48] and the Biopolymer module of Sybyl[52] as described previously.[46]

Docking and MD Simulation

In the next step dDAVP was docked into the V2R–Gs_{α}(382–394), V1aR– $Gq/11_{\alpha}$(347–359), and OTR–$Gq/11_{\alpha}$(347–359) systems, using a modified genetic algorithm as implemented in AutoDock program.[54] AutoDock is a suite of programs designed to predict the bound conformation(s) of a flexible ligand to a macromolecular target.[54,56] Details of the docking procedure were described elsewhere.[14,56,57] The relaxation of the complexes using a constrained simulated annealing (CSA) protocol in vacuo for 15 ps,[53] followed by energy minimization, with positional constrains on C_{α} atoms in 7TM to maintain the receptors shape in homology to MII was done. The two lowest-energy systems per each V2–Gs_{α}(382–394)–dDAVP, V1a–$Gq/11_{\alpha}$(347–359)–dDAVP, and OTR–$Gq/11_{\alpha}$(347–359)–dDAVP complex were chosen. Subsequently, six selected complexes were inserted into the fully hydrated 1-palmitoyl-2-oleoyl-*sn*-glycero-3-phosphatidylcholine (POPC) membrane model.[58,59] No additional water molecules were placed inside the receptor cavity. The models were submitted to the MD simulation in the Amber 7.0 force field,[48] using particle-mesh Ewald electrostatic summation[60] as already described.[14] Briefly, the periodic box of each complex consisted of 120 POPC lipid molecules, over 3,500 water molecules, and Cl^{-} counterions. Moreover, for all components of complexes, the OPLS[61] united atom parameters were applied. The flat-bottom soft harmonic-wall restraints were imposed onto the φ, ψ, and ω peptide angles of the 7TM amino acid residues to avoid unfolding or any other unwanted modifications of the helices. In accordance with the standard Amber protocol, the positional TM C_{α}

constraints were used exclusively for the first 100 ps of the simulation during heating the system from 0 to 300 K to prevent the helices from degeneration. From 100 to 1,000 ps free MD simulation without positional constraints was carried out. Finally, the energy minimization of the 1-ns MD snapshots in the Amber 7.0 force field[48] was done.

Analysis of Interactions and Supplementary MD

After MD simulation six relaxed complexes were obtained. For analysis of the receptor–ligand interactions, one lower energy complex for each receptor was selected. It has been experimentally demonstrated that the D103 located in the EL1 of V2R determines the high affinity binding of the dDAVP.[38] Unfortunately, in both V2R–dDAVP complexes this interaction did not appear, neither during docking nor during unconstrained MD. Thus, we attempted the supplementary manual docking of the dDAVP in V2R using a Swiss–PdbViewer.[62] The previously selected (that of lower energy) dDAVP–V2R complex was slightly modified via displacement of ligand molecule toward the EL1 to serve as input for a new 1-ns MD. Therefore, the D-Arg^8 side chain was situated proximal to EL1 D103, while the cyclic part of the molecule was retained docked in the depth the binding cavity within the 7TM domain (see Figure 1). Subsequently, the complex was relaxed by the CSA protocol followed by the energy minimization and submitted to the 1-ns MD simulation in hydrated membrane analogously as described above and subsequently used for analysis of V2R–dDAVP interactions. Actually, dDAVP was partially "undocked" by being pulled out toward the extracellular side and slowly docked again during MD, resulting in the second V2R–dDAVP complex. It is impossible to observe a course of the docking in AutoDock, where the ligand is instantly generated in the optimal location inside the binding cavity, thus the AutoDock-produced complexes represent the final states of docking. The slow ligand docking during 1-ns MD might stand for model of the docking course. Therefore, the supplementary V2R–dDAVP complex might represent one of early states of docking.

Receptor amino acid residues involved in ligand binding have been identified using distance criteria, i.e., all amino acid residues in which any atom was not farther away than 3.5 Å from any atom of the dDAVP residue, were chosen to be interacting. Subsequently all receptor residues not involved in any interaction were omitted during visual inspection. Several distant residues interacting with the ligand were added on condition that they were not farther away than 4.5 Å. The amino acid residues meeting these criteria are listed in Table II. The most essential interactions between dDAVP and respective receptors are characterized by visual inspection and are presented in Figure 2.

Nomenclature

The dDAVP residues are identified using three-letter codes with the indices in parentheses, e.g., D-Arg^8, while the receptor residues are identified using one-letter codes with the universal Class A indices (Ballesteros–Weinstein numbering scheme)[63] placed as superscripts, followed by the absolute numbers and e.g., V2R E$^{1.35}$40. In the Ballesteros–Weinstein scheme, the most conserved residue in the TM helix 'N' has been given the number 'N'50, and each residue is numbered according to its position relative to this conserved residue. Residues placed in loops are identified with a one-letter code, followed only by the residue absolute number e.g., EL2 V189.

Moreover, in describing receptor–ligand interactions involving the three-component names of complexes, e.g., "V2R–dDAVP–Gs$_\alpha$(382–394)," the clause "Gs$_\alpha$(382–394)" is omitted for better legibility. Telling about the receptor–G protein interaction, the name of the G protein segment e.g., "Gs$_\alpha$(382–394)" is abbreviated to "Gs$_\alpha$." The G protein residues are identified a using one-letter code following the name of G protein class e.g., Gs$_\alpha$ L393.

Two V2R–dDAVP complexes are marked as I and II (AutoDock and manual docking, respectively).

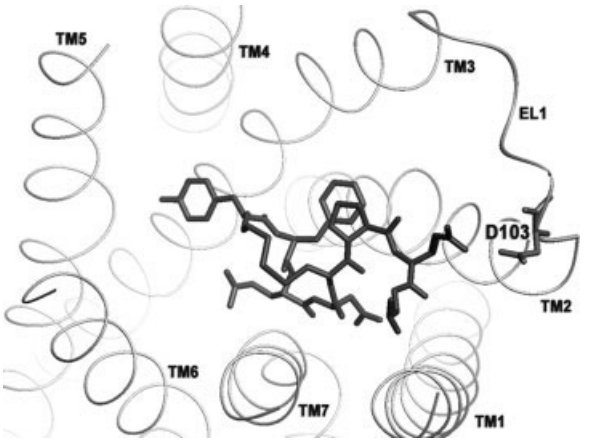

FIGURE 1 dDAVP docked to the V2R cavity after manual docking, before MD. The D-Arg^8 side chain is situated proximal to EL1 D103, while the cyclic part of the molecule remains docked in the depth the binding cavity within the 7TM domain. The figure was prepared using the program RasMol.[115]

RESULTS AND DISCUSSION

Conformation of Receptors and dDAVP and Their Changes during MD

The binding pockets of the dDAVP in all receptors are formed within TM1–TM7 with the ligand located perpendicularly to the longer axis of the receptor (see Figure 2). All receptor–dDAVP complexes remained stable during 1-ns unconstrained MD and there were insignificant conformational changes of the receptor structures. The RMSD measured on the all atoms/

Table II List of the V2R, V1aR, and OTR Residues Directly Involved in the Interactions with dDAVP[a]

TM 'N' domain	V2R(I)	V2R(II)	V1aR	OTR	Universal numbering	Experimental data (Ref.)
N terminus	R32	R32	R46	R34	—	68, 69
TM1	E40	E40	E54	E42	1.35	70
	L44	L44	L58	L46	1.39	70, 97
TM2	V88	V88	—	—	2.53	92
	Q92	Q92	Q104	—	2.57	64, 99, 100
	—	V93	—	V93	2.58	99
	Q96	Q96	Q108	Q96	2.61	64
	W99	W99	W111	W99	2.64	73
	—	—	D112	D100	2.65	95
TM3	V115	V115	V127	—	3.28	101
	—	K116	K128	K116	3.29	64, 100, 101, 102
	Q119	Q119	Q131	Q119	3.32	64
	M120	—	V132	V120	3.33	—
	M123	M123	M135	M123	3.36	—
	—	—	F136	F124	3.37	—
	S127	S127	—	—	3.40	—
TM4	—	—	Q185	Q171	4.60	64, 100
	—	Q180	M191	—	4.66	—
EL2	R181	R181	I192	R178	—	105 (V2R)
	—	S187	—	—	—	—
	—	G188	K199	—	—	—
	V189	V189	A200	—	—	—
	T190	T190	R201	F185	—	—
	C192	C192	—	—	—	—
TM5	—	—	Y216	Y200	5.38	—
	V206	V206	V217	I201	5.39	103 (V2R)
	I209	I209	M220	I204	5.42	92 (V2R)
	—	A210	—	—	5.43	—
	V213	—	I224	V208	5.46	—
	F214	F214	F225	—	5.47	104
TM6	F287	F287	F307	F291	6.51	102
	Q291	Q291	Q311	Q295	6.55	64
	A294	—	S314	S298	6.58	92 (V2R)
TM7	—	F307	—	F311	7.35	—
	V308	V308	T331	I312	7.36	—
	M311	M311	A334	M315	7.39	—
	—	L312	L335	L316	7.40	—
	—	A314	G337	A318	7.42	—
	S315	S315	S338	S319	7.43	65

[a] The majority of residues conserved in the vasopressin/oxytocin family were previously experimentally determined as crucial for ligand binding. Among the non-conserved residues, for residues determined in V2 receptor subtype, the receptor name is given in parentheses.

7TM C_α atoms were 3.45 Å/2.48 Å for V2R(I), 1.62 Å/1.26 Å for V2R(II), 2.64 Å/1.79 Å for V1aR, and 2.91 Å/2.88 Å for OTR. The lower RMSD for V2R(II) is not surprising and results from better relaxation of the input receptor structure, which was previously simulated for 1 ns as opposed to remaining complexes (see Analysis of Interactions and Supplementary MD). Moreover, strong receptor–ligand interactions (see below) contribute to the stability of the complex. Finally, there are very similar dDAVP conformations in both V2R–dDAVP(I) and V2R–dDAVP (II) complexes with only the exception of D-Arg[8] location as shown in Figure 2. In general, the location of dDAVP is nearly identical in all complexes contrary to the dissimilar AVP location observed in the same receptors, as described in our previous work.[47] The location and conformation of dDAVP change somewhat during MD in all receptors, mostly in OTR, and the RMSD measured on the C_α atoms of dDAVP are: 1.15 Å in V2R(I), 0.74 Å in

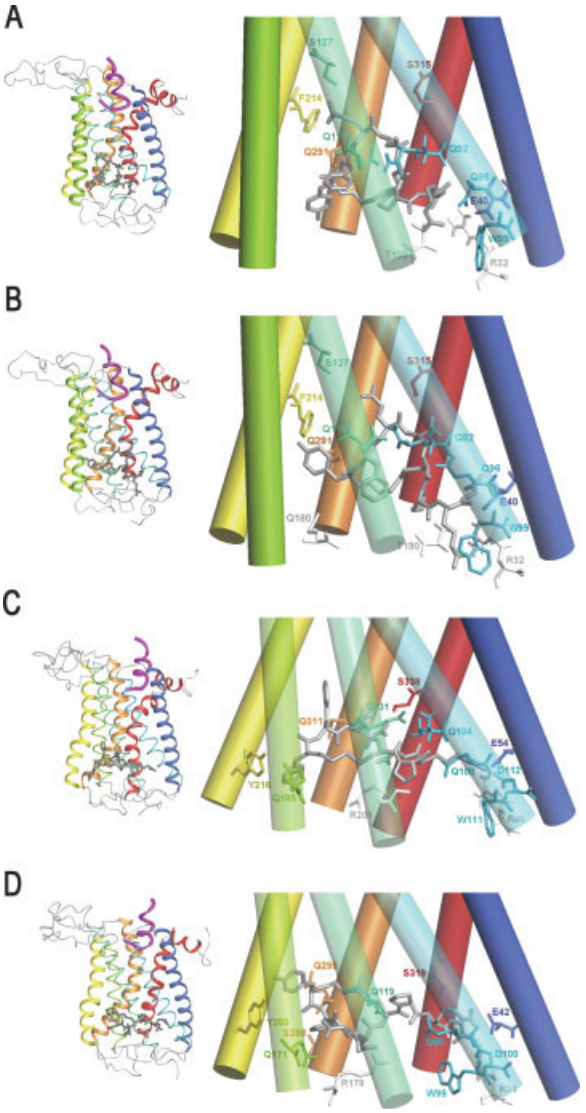

FIGURE 2 Representation of the dDAVP binding pockets in neurohypophyseal hormone receptors. (A) V2R(I), (B) V2R(II), (C) V1aR, (D) OTR. The TM helices are colored from blue (TM1) to red (TM7), the dDAVP is gray, the G_α protein C-terminal peptide is magenta. Several helices are drawn thinner or transparently for clarity. Left: the location of the ligand and G protein segments inside their binding cavities is shown. Right: the binding amino acid residues are marked and their side chains are exposed; they are colored in agreement with the TM to which they belong while the EL2 residues are gray. The extracellular loops are omitted for clarity. The figure was prepared using the program MolMol.[116]

V2R(II), 1.45 Å in V1R, and 2.48 Å in OTR. The lower RMSD for ligand molecule in V2R(II) results from their better relaxation before docking. The low RMSD values for both the ligand and the receptor show stability of the whole complex. In all investigated receptors the γ-turn is formed in the ligand molecule and the stability for dDAVP conformation is provided via one hydrogen bond between peptide backbone, i.e., the carbonyl oxygen of Mpa^1 interacts with the Phe^3 amide proton. Furthermore, the C-terminal part of molecule, i.e., the important guanidinium group of D-Arg^8 is located within TM1–TM3. However, in the V2R–dDAVP (II) complex, the D-Arg^8 side chain projects outside the 7TM core, whereas in V2R-dADVP(I) it is more embedded by the binding cavity. In all complexes the N-terminal part with the Tyr^2 and Phe^3 aromatic rings is situated near TM5–TM6, but in no complex do they interact with each other, as a consequence of Tyr^2 with respect to Phe^3 location on the opposite sides of the macrocyclic ring plane in the V1aR–dDAVP and OTR–dDAVP complexes. Similarly, in both V2R–dDAVP complexes the Phe^3 side chain is situated perpendicularly to the plane of the tocin ring, since there is also no chance for stacking interaction with Tyr^2. In Figure 3 the superposition of dDAVP structures before and after MD simulations is presented. In the V2R–dDAVP(I) complex, three other intramolecular hydrogen bonds between side chains are formed in the ligand molecule. Therefore, the Cys^6 carbonyl oxygen simultaneously interacts with the D-Arg^8 amide and Asn^5 carboxamide protons. Moreover, the Pro^7 carbonyl oxygen interacts with the D-Arg^8 guanidinium. As a result of forming the hydrogen bonds involving side chains of Asn^5 and D-Arg^8, they are slightly weaker when exposed to interactions with the receptor residues, contrary to the fully accessible Gln^4 and the C-terminal carboxamides. In the V2R–dDAVP(II) complex, only one intramolecular hydrogen bond present in the V2R–dDAVP(I) complex has been retained, hence, the Cys^6 carbonyl oxygen still interacts with the D-Arg^8 amide proton. As a result of the lack of other hydrogen bonds involving the polar side chains in V2R–dDAVP, they are fully accessible for interactions with the receptor residues. In both dDAVP–V2R complexes, the aromatic side chain of Tyr^2 is well exposed for interaction with the receptor, whereas, in the dDAVP–V2R(II) complex, the Phe^3 aromatic ring, slightly dislocated over the macrocyclic ring, is less accessible for receptor residues. The most significant conformational change observed in the dDAVP–V2R(I) complex during 1-ns MD is the dislocation of D-Arg^8 side chain and formation of hydrogen bond with Pro^7 as described above (see Figure 3A). The situation of the remaining side chains has also changed, mainly that of Gln^4 and Pro^7. In the V2R–dDAVP(II) complex, the location of all side chains changes only to a small extent (see Figure 3B), however, mainly for Gln^4, as in the former com-

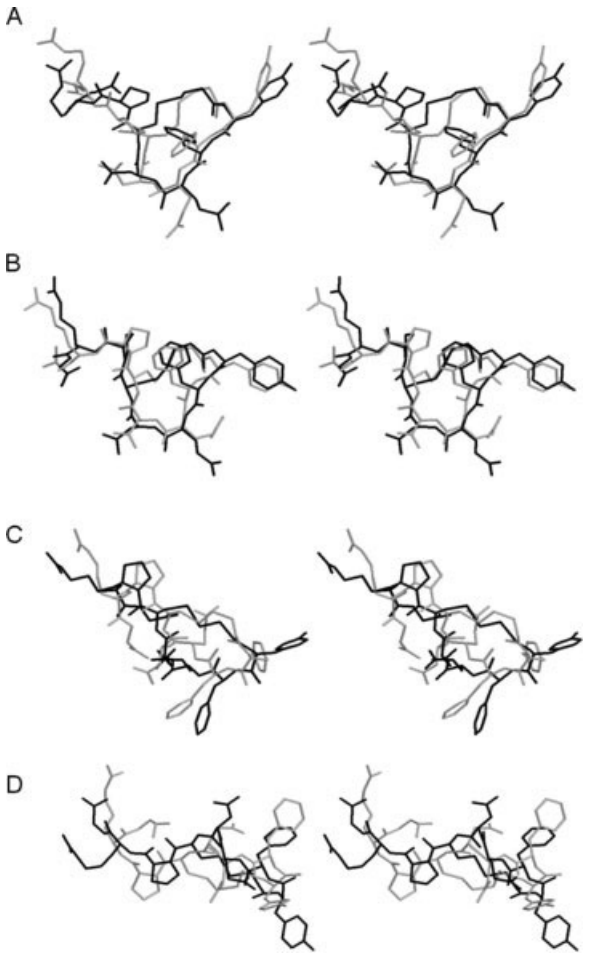

FIGURE 3 Stereodiagrams of superimposition of the dDAVP conformations inside the respective receptors before (gray) and after (black) MD. (A) V2R(I), (B) V2R(II), (C) V1aR, (D) OTR. The figure was prepared using the program RasMol.[115]

plex. In the V1aR–dDAVP complex, one more intramolecular hydrogen bond can be observed involving the Asn^5 amide oxygen and the C-terminal carboxamide proton, thus the latter group is less accessible for interaction with the receptor than the other side chain groups. The Asn^5 side chain is folded back beneath the ring moiety toward the disulfide bridge and this is the most important change during 1-ns MD along with the displacement of the Gln^4 side chain (see Figure 3C). In the complex with OTR, one more hydrogen bond also can be formed, between the Phe^3 carbonyl oxygen and the Gln^4 amide proton (see Figure 3D), resulting in a poor accessibility of this group for OTR residues. Moreover, in this complex, the location of all side chains changes noticeably during MD in agreement with the highest RMSD for dDAVP in OTR.

V2R–dDAVP Complexes

Influence of Highly Conserved Residues Interacting with dDAVP on Receptor Activation. In Figure 2A and B and Table II, the most noticeable V2R–dDAVP interactions are given. The network of many hydrogen bonds involving the conserved amino acid residues (see multiple sequence alignment in Figure 4) can be observed in both V2R–dDAVP(I) and V2R–dDAVP(II) complexes. The interactions involving the highly conserved 7TM Gln residues ($Q^{2.57}92$, $Q^{2.61}96$, $Q^{3.32}119$, and $Q^{6.55}291$) seem to be especially important for ligand binding. This is not surprising since they make a part of the binding cavity, moreover, their side chain carboxamide could either be a donor or an acceptor of hydrogen bonds formed with the ligand. Therefore, the Gln carboxamides could form the hydrogen bonds with the polar side chains group of dDAVP as follows: $Q^{2.57}92$–Asn^5; $Q^{2.61}96$–D-Arg^8, and $Q^{6.55}291$–Tyr^2, identically in both V2R–dDAVP complexes with the exception of $Q^{3.32}119$ interacting with Asn^5 and Gln^4 in V2R–dDAVP(I) and V2R–dDAVP(II) complexes, respectively. The conserved 7TM Gln residues have been first recognized as responsible for binding neurohypophyseal hormones and their analogs to rat V1aR.[64] Moreover, their importance for OT and AVP binding in human neurohypophyseal hormone receptors has been proposed.[46,47] The detailed examination of obtained receptor models, both inactive and active, may explain their function. In the model of the inactive receptor, constructed on the template of RD crystal structure,[5,16] the $Q^{2.57}92$, $Q^{2.61}96$, and $Q^{3.32}119$ carboxamides interact via hydrogen bonds with another highly conserved residue $S^{7.43}315$ (see Figure 5A). This interaction is broken in the agonist-bound model, as a result of interaction of these three Gln residues with dDAVP as described above (see Table II and Figure 2). Moreover, $S^{7.43}315$ also interacts with the ligand via its hydroxyl forming the hydrogen bond with the backbone carbonyl of Asn^5 or Gln^4 in V2R–dDAVP(I) and V2R–dDAVP(II) complexes, respectively. Accordingly, S315R mutation in V2R has been identified as being responsible for NDI by impairing AVP binding.[65] The docking of ligand may directly break the interaction between three Gln and $S^{7.43}315$ as an internal constraint between TM2, TM3, and TM7 and consequently result in their rearrangement, which is believed to be part of the activation process.[12] There are several reasons that may support this hypothesis. First of all, for the human β_2 adrenergic receptor, it has been proposed that two equivalent residues, $Y^{7.43}316$ and $D^{3.32}113$, interact with each other in the unoccupied receptor model and

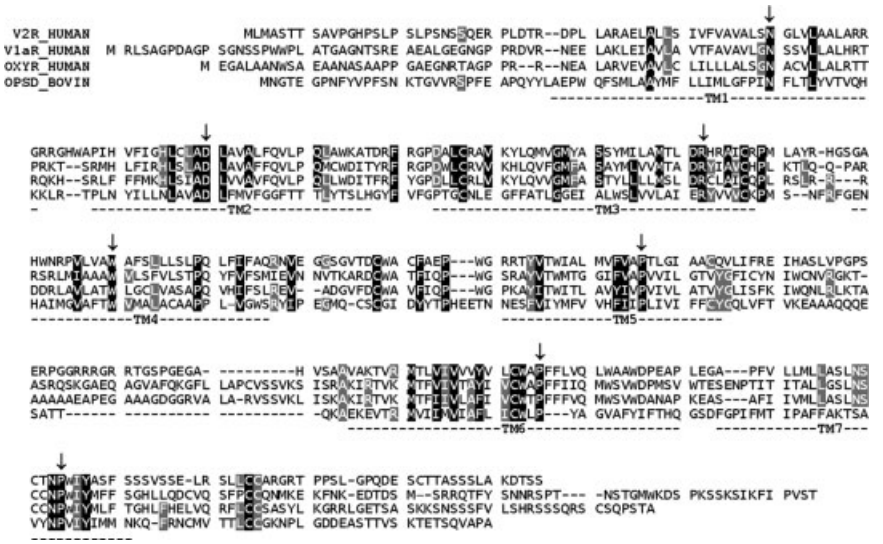

FIGURE 4 Primary sequence alignment of the human neurohypophyseal hormone receptors (OTR, V1aR, and V2R) and bovine rhodopsin, obtained using Multalin.[117] The putative transmembrane helices 1–7 are underlined. The conservative residues, indicative of high-level similarity within the subfamily, are shown in black while those with lower-level similarity are shown in gray.[25] The TM 'N'50 residues are marked with an arrow.[63]

this interaction is absent in the agonist–receptor complex.[66] Second, it is also noticeable that $S^{7.43}315$ is equivalent to RD $K^{7.43}296$ (see sequence alignment, Figure 4), where the $K^{7.43}296$–$E^{3.28}113$ salt bridge maintains RD in the inactive state.[67] In the vasopressin/oxytocin receptor subfamily, the valyl ($V^{3.28}$) is conserved at this position and $Q^{2.57}92$, $Q^{2.61}96$, and $Q^{3.32}119$ are the only residues in this region that possess polar side chains long enough to form the interhelical interaction (see sequence alignment, Figure 4).

Two other highly conserved V2R residues, R32 and $E^{1.35}40$, located in the N-terminus and TM1, respectively, might be involved in ligand recognition. In both complexes their oppositely charged side chain groups form a salt bridge with each other and interact with the ligand simultaneously. In the V2R–dDAVP(I) complex, the C-terminal carboxamide of dDAVP is headed toward R32 guanidinium in the N-terminal sequence, whereas in the V2R–dDAVP(II) complex it is located closer to the $E^{1.35}40$ carboxyl. Indeed, the C-terminal carboxamide might interact with both residues forming an ionic pair at the same time. The equivalent arginyl (R46 and R34 in V1aR and OTR, respectively) has been identified as playing a critical role in high-affinity agonist binding.[68,69] In addition, $E^{1.35}46$ has been recently determined to be critical for AVP binding in V1aR.[70] The molecular basis for the significance of these two residues has not been defined; however, it has been suggested that it could be involved in the intramolecular interactions with negatively charged residues.[69,70] Molecular modeling in this study may help to explain this mechanism. In the inactive state of V2R, the R32 side chain is exposed toward the extracellular side and forms a salt bridge with the conserved EL3 E303 (see Figure 5B). Differently, in the agonist-bound model (V2R–dDAVP(I) complex), the R32 side chain is dislocated toward the binding cavity and interacts with the $E^{1.35}40$ carboxyl (see Figure 5C). Furthermore, this ionic pair strongly interacts with the C-terminal carboxamide of dDAVP, as described above. Accordingly, it has been demonstrated that the deletion of C-terminal carboxamide results in AVP analogs with low agonist activity.[71] It is conceivable that dDAVP approaching from the extracellular side might interact directly via C-terminal carboxamide with highly exposed R32, resulting in dislocation of its side chain toward the binding cavity along with the docking ligand. This interaction would result in the disruption of the R32–E303 salt bridge linking TM1 and TM7 and triggering the conformational changes leading to receptor activation. Interestingly, in the V2R–dDAVP(II) complex the R32 interacts with these both aspartates simultaneously (Figure 5D). This might be a model of the intermediate state, resulting from the slower docking during MD, contrary to instant docking in AutoDock (see Analysis of Interactions and Supplementary MD).

The highly conserved $W^{2.64}99$ interacts with the D-Arg[8]; however, in the V2R–dDAVP(I) complex these residues are situated perpendicularly to each other in

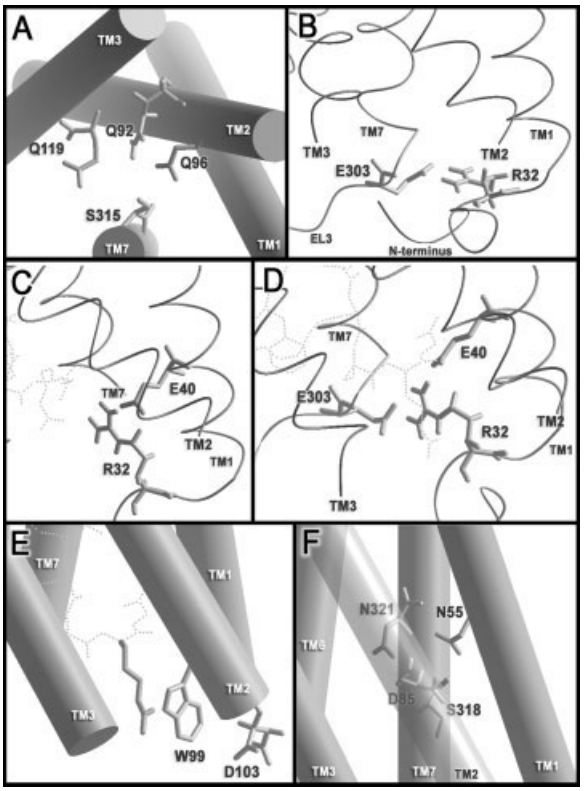

FIGURE 5 Representation of some interactions crucial for the V2R activation or ligand binding. The TM helices are signed and crucial receptor residues are exposed; the ligand is marked with dotted lines. (A) The interhelical interactions between the conserved residues stabilizing the inactive V2R. (B–D) The interactions involving the highly conserved arginyl observed in the inactive V2R, V2R–dDAVP(I) complex, and V2R–dDAVP(II) complex, respectively. (E) The location of $W^{2.64}99$ after MD in V2R–dDAVP(II) complex resulting in the disruption of the salt bridge between D-Arg^8 and EL2 D103; the dDAVP D-Arg side chain is thicker for clarity. (F) The interhelical interaction of the highly conserved residues involved in the receptor activation; the TM2 is transparent for clarity. The figure was prepared using the programs RasMol[115] and MolMol.[116]

contrast to their exactly parallel arrangement in the V2R–dDAVP(II) complex. The hydrogen bond is formed between the $W^{2.64}99$ indole and D-Arg^8 guanidinium in the V2R–dDAVP(I) complex. The model of interaction of these two planar groups observed in the V2R–dDAVP(II) complex has been recognized as being energetically favorable[72] and might be directly involved in the ligand dislocation toward the bottom of the binding cavity (see below). Furthermore, a W99R mutation has been identified in NDI patients and oligonucleotide-directed mutagenesis revealed that $W^{2.64}$ is involved in high-affinity binding of agonists to the V2R.[73] The remaining conserved residues interacting with the dDAVP (see Table II) in our models do not seem to be as important as the residues described above. Some of the hydrophobic residues, especially those with bulky side chains, may play a role in proper positioning of important receptor residues, such as two conserved valyl residues: $V^{2.53}88$ and $V^{3.28}115$. These two residues, in an inactive receptor, form the steric constraints delimiting the conformational space of crucial $Q^{2.57}92$ (partially also $Q^{3.32}119$). Therefore, they might force the appropriate Gln position to form the interhelical interaction with $S^{7.43}315$ as described above and shown in Figure 5A.

Nonconserved Residues Are Involved in the V2R–dDAVP Selectivity. As described under Methods, the dDAVP molecule was "redocked" with manual help to form the salt bridge between D-Arg^8 guanidinium and EL1 D103 (see Figure 1). Unexpectedly, after 1-ns MD this interaction was discontinued. The analysis of the MD trajectory revealed slow relocation of $W^{2.64}99$ indole between D-Arg^8 and D103 until disruption of the previously formed salt bridge as shown in Figure 6. The exactly parallel arrangement of indole $W^{2.64}99$ and D-Arg^8 guanidinium in the final complex (see Figure 5E) prevents any interaction of the latter with EL1 D103 carboxyl. Nevertheless, it does not necessarily contradict the experimental results, in which the EL1 D103 was identified as a residue crucial for high affinity V2R–dDAVP binding

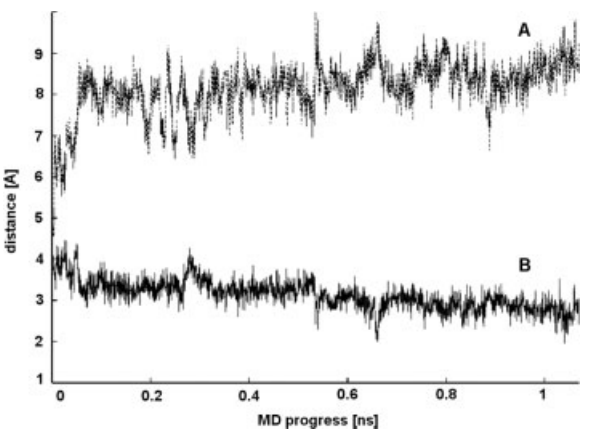

FIGURE 6 Representation of the $W^{2.64}99$ dislocation disrupting the D-Arg^8–D103 salt bridge observed during MD. All distances has been measured from the centers of gravity of the side chain heavy atoms. (A) Distance between the D-Arg^8 and D103 side chains. (B) Distance between the $W^{2.64}99$ and half of the hypothetical line connecting the D-Arg^8 and D103.

and proposed to interact with D-Arg^{8}.[38] Therefore, the D-Arg^{8}–D103 salt bridge might be formed at the recognition stage, before dDAVP entry into the V2R binding pocket. Subsequently, the interaction would slowly disappear during docking, thus making possible a correct, deep immersion of ligand inside the binding cavity leading to full receptor activation.

Other interactions are probably less important. The interactions involving the nonconserved 7TM residues and Gln^{4} and Tyr^{2} of the ligand can be observed. In both complexes the S$^{3.40}$127 hydroxyl might form a hydrogen bond with the Gln^{4} carboxamide, whereas F$^{5.47}$214 might interact with the Tyr^{2} and/or Gln^{4} side chains. The interaction between the C-terminal carboxamide and V$^{7.36}$308 can be observed in both complexes. Moreover, the second extracellular loop strongly interacts with the C-terminal part of the ligand. Thus, in the V2R–dDAVP(I) complex, the EL2 T190 hydroxyl may form hydrogen bonds with the C-terminal carboxamide, the Gly^{9} amide proton, and the D-Arg^{8} guanidinium simultaneously. Similar interaction can be observed in the V2R–dDAVP(II) complex, where the EL2 T190 hydroxyl may form a hydrogen bond with the C-terminal carboxamide of dDAVP. The aromatic–hydrophobic interactions between M$^{3.33}$120, V$^{5.39}$206, I$^{5.42}$209 and aromatic rings of Tyr^{2} and Phe^{3} take place; furthermore, M$^{7.39}$311 interacts with the dDAVP disulfide bridge. In any V2R–dDAVP complex aromatic π–π receptor–ligand interactions have not been observed, in agreement with the hypothesis that they are involved in stabilization of an inactive state of the receptor, as previously proposed.[15,16,74]

Interaction with the Gs$_\alpha$(382–394) C-terminal Peptide. To identify the V2R–Gs$_\alpha$(382–394) interactions, any receptor and Gs$_\alpha$ residues within the mutual distance of 4.0 Å or less have been selected and subjected to detailed analysis. The receptor residues identified as interacting with the Gs$_\alpha$ segment are shown in Table III and Figure 7. In both V2R–dDAVP(I) and V2R–dDAVP(II) complexes these interactions are identical. This is not surprising, since the location of Gs$_\alpha$(382–394) and its interaction with V2R remained unchanged during the renewed docking of dDAVP (see Methods). Subsequent 1-ns MD has not had any effect on their interactions.

The residues involved in the receptor–Gs$_\alpha$ interaction are prevailingly hydrophobic; however, a few significant polar contacts occur. The important polar interactions seem to be two salt bridges formed by R$^{3.50}$137 and D$^{3.49}$136 from the highly conserved (D/E)RY (in V2R : DRH) motif at the cytoplasmic end of TM3. In our model the D$^{3.49}$136 carboxyl interacts with the Gs$_\alpha$ R389 guanidinium, while the R$^{3.50}$137 guanidinium might interact with the Gs$_\alpha$ L394 C-terminal carboxyl and/or Gs$_\alpha$ E392 carboxyl. Moreover, the same Gs$_\alpha$ E392 interacts with the carboxamides of the highly conserved N$^{7.45}$317 and N$^{7.49}$321 via hydrogen bonds as well as the another hydrogen bond that may be formed between the Y$^{7.53}$325 hydroxyl and the Gs$_\alpha$ Q390 carboxamide. R$^{3.50}$137 has been recognized to play a key role in triggering G protein activation and mutation of this residue to histidine in the human V2R totally abolishes V2R–Gs coupling, resulting in a complete type of NDI.[75] Mutation of the R$^{3.50}$ in OTR and several other receptors has established an important role of this residue in G protein activation.[76–79] Accordingly, it has been suggested that the substitution of the adjacent acidic residue (Glu or Asp in D/ERY motif) with noncharged residue leads to constitutive activity.[80–82] However, it has been recently demonstrated that the arginyl of the DRY motif is not essential for G protein coupling for a novel wild-type receptor, ORF74-EHV2.[83] Hence, although this motif is highly conserved, its function in the GPCR activation and signaling might be specific for particular receptors.[84] The N$^{7.49}$321 and Y$^{7.53}$325 are the part of highly conserved NPxxY motif at the cytoplasmic side of TM7; mutations of N$^{7.49}$ in different GPCRs have revealed that this residue is involved either in the adenylyl cyclase or in the phospholipase C activation.[85–87] Moreover, the analysis of the inactive V2R model reveals that N$^{7.49}$321 participates in the network of the interhelical hydrogen bonds, involving the highly conserved residues N$^{1.50}$55, D$^{2.50}$85, and S$^{7.46}$318 (see Figure 5F). Interestingly, S$^{7.46}$318 interacts simultaneously with S$^{7.43}$315, which is involved in the interhelical interaction with three Gln residues, as already described (see Figure 5A). Therefore, it is possible that the docking of agonist not only breaks the interaction between three Gln and S$^{7.43}$315, as proposed previously, but initiates a gradual disruption of the interhelical hydrogen bond network during receptor activation, finally leading to the N$^{7.49}$321 side chain rearrangement toward the intracellular side for interaction with Gs$_\alpha$(382–394); as shown in the V2R–dDAVP complexes (Figure 7). An activation mechanism involving N$^{7.49}$ has been recently proposed for thyrotropin receptor.[88]

The remaining interactions at the receptor–Gs$_\alpha$(382–394) interface are hydrophobic. The most important handle point seems to be the highly conserved Gs$_\alpha$ L393, interacting with as many as five V2R residues: I$^{2.43}$78, L$^{2.46}$81, M$^{3.42}$129, I$^{3.43}$130, and M$^{3.46}$133 (see Figure 7). Less important hydrophobic interactions can also be observed, involving

Table III List of the V2R, V1aR, and OTR Residues Involved in the Interaction with the G_αC-Terminal Segments

	V2R(I, II)	V1aR	OTR	Universal numbering
TM1	L57	S71	—	1.52
	V58	V72	V60	1.53
	A61	A75	A63	1.56
	R65	T79	T67	1.60
IL1	—	K82	K70	—
TM2	P73	—	—	2.38
	I74	M86	L74	2.39
	F77	F89	F77	2.42
	I78	I90	M78	2.43
	L81	—	—	2.46
TM3	M129	M141	—	3.42
	I130	—	L130	3.43
	A132	—	—	3.45
	M133	M145	M133	3.46
	D136	D148	D136	3.49
	R137	R149	R137	3.50
	A140	—	—	3.53
	I141	—	I141	3.54
IL2	Y148	—	—	—
TM6	—	R288	R272	6.32
	—	—	M276	6.36
	—	—	I279	6.39
	—	—	I280	6.40
	—	—	F284	6.44
TM7	N317	—	—	7.45
	S318	—	—	7.46
	N321	N344	N325	7.49
	P322	P345	P326	7.50
	Y325	Y348	Y329	7.53
			T333	7.57
C-terminus	—	—	L336	—
	—	L356	F337	—
	—	V360	—	—
	—	F363	—	—

the highly conserved Gs_α L388, interacting with $I^{2.39}74$ and $F^{2.42}77$. These two Gs_α Leu residues, L388 and L393, are conserved among members of functionally different G protein classes[42] and have been recognized as being absolutely crucial for receptor–G protein binding.[89–91] Moreover, the nonconserved C-terminal Gs_α L394 interacts with $A^{3.45}132$ and $M^{3.46}133$ while the Gs_α Y391 interacts with $P^{7.50}322$ and $Y^{7.53}325$ again from the NPxxY motif. Accordingly, the mutation of $P^{7.50}322$ has been identified in NDI, resulting in a V2R mutant having impaired its ability to mediate the activation of adenylyl cyclase.[92]

Described V2R–Gs_α(382–394) interaction involves the conservative residues of both interacting individuals: DRY and NPxxY motifs from receptor and two highly conserved leucyls from the G protein. These interactions have been formed at the step of activated models building,[46] while subsequent MD simulation with dDAVP applied in this study allows better fitting of the receptor–G protein interacting parts and strengthening of the existing interactions. Hence, it is a reasonable validation of our recent hypothesis concerning the interaction of class A GPCRs with G proteins.[45]

The Role of Internal Water Molecules. Internal water molecules, contributing to the intricate network of hydrogen bonds inside the receptor, involving the dDAVP and Gs_α(382–394), have accumulated during

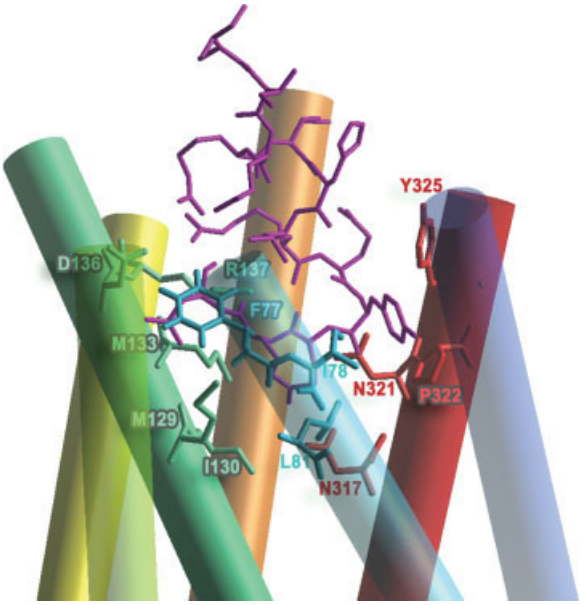

FIGURE 7 Gs_{α}(382–394) docked inside the intracellular cavity of V2R. The TM helices are colored from blue (TM1) to red (TM7); the G protein is magenta. TM1–TM3 are made transparent for clarity; the interacting V2R resides are exposed. The figure was prepared using the program MolMol.[116]

the productive MD simulation. As described under Methods, no water molecules were intentionally located inside the receptor, nonetheless water molecules, hydrating the lipid bilayer, migrated into the receptor cavity during the simulation. The water molecules escaped the hydration layer after approximately 50 ps of MD and remained at their target positions through the rest of the simulation (see Figure 8).

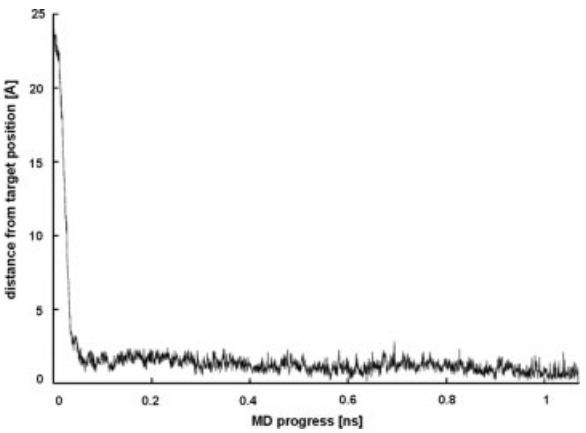

FIGURE 8 The dislocation of a specimen water molecule escaping the hydration layer. The water molecules enter inside the receptor cavity at the very beginning of the MD and remain at approximately the same (final) position over the whole simulation.

In both V2R–dDAVP complexes water molecules interact mainly with the polar residues having well-exposed long side chains, which makes it favorable binding site for an H-bond donor/acceptor. In Figure 9, several water-mediated interactions exemplifying their structural function and a role in stabilization of the receptor agonist-bound state are depicted. The most important ones appear to be the interhelical interactions that can be formed due to mediating water molecules. Therefore, as one may see in Figure 9A, this particular interaction might have an influence on the rearrangement of the adjacent parts of TM1, TM2, and EL2, where the interacting residues of the receptor belong. This interaction may contribute to forming the protuberance of EL2 projecting toward the extracellular side as observed in the activated state (Figure 2). Some of the identified water mole-

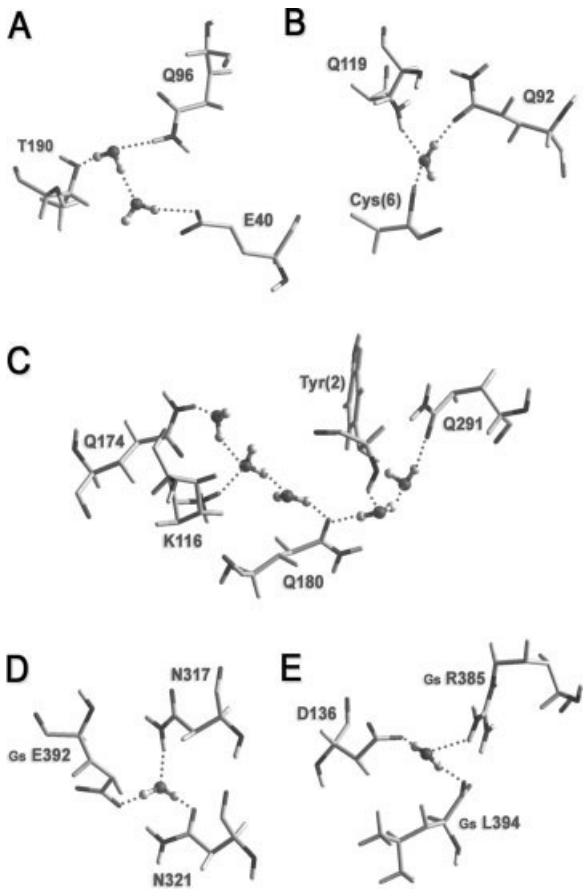

FIGURE 9 Representation of the water-mediated interactions exemplifying their structural function and role in stabilization of the receptor agonist-bound state (for details see The Role of Internal Water Molecules). The figure was prepared using the program MolMol.[116]

cules, located within the receptor–ligand contact surface, may mediate the receptor–ligand indirect interactions (e.g., see Figure 9B and C). In Figure 9B, one may see an interaction of one water molecule with two receptor residues and one ligand residue. This interaction might have an influence on the correct position of two highly conserved Gln, $Q^{2.57}92$ and $Q^{3.32}119$, which, apart from water-mediated interaction with Cys^{6} backbone, could interact with the ligand directly (see Figure 2A and B). The largest cluster consisting of five water molecules mediates the interaction with as many as four receptor and one ligand residues as shown in Figure 9C. Therefore, three receptor domains, TM3 ($K^{2.29}116$), TM4 ($Q^{4.60}174$, $Q^{4.66}180$), and TM6 ($Q^{6.55}291$), are involved in an interhelical water-mediated hydrogen bond network. Moreover, the Tyr^{2} backbone also participates in these stabilizing interactions. It is noticeable that in our model highly conserved $Q^{4.60}174$ and $K^{2.29}116$ interact with the dDAVP only due to mediation of water molecules, but not directly. Both of these residues, along with $Q^{6.55}291$, are believed to be crucial for ligand binding,[64] whereas the nonconserved $Q^{4.66}180$ has been proposed as being responsible for selective binding to V2R.[47] The network of water molecules can be also observed within receptor–Gs_{α} contact surface (Figure 9D and E). These interactions also contribute to the stabilization of the whole complex. In Figure 9D, one water molecule mediating the interaction between Gs_{α} E392 and two receptor residues, $N^{7.45}317$ and $N^{7.49}321$, is shown. A similar interaction is shown in Figure 9E, where two Gs_{α} residues, R385 and L394, interact via one water molecule with the highly conserved $D^{3.49}136$. As can be seen in Figure 9E, at the receptor–G protein contact surface long water bridges also can be formed. It is shown that the S333 from the C-terminus of V2R does not interact with the Gs_{α} directly.

The structure and function of internal water molecules in GPCR is still little known contrary to their well-defined function in bacteriorhodopsin.[93,94] Yet, water molecules identified in the vicinity of highly conserved residues in the RD crystal structure have been proposed to control the activity of RD and other class A GPCRs.[7] Selected water-mediated interactions presented in this section demonstrate fairly well their possible contribution to the stabilization of the V2R–dDAVP–Gs_{α} complexes. The detailed examination of several different complexes of vasopressin and oxytocin receptors, both in antagonist- and agonist-bound states, supporting the hypothesis about the structural function of internal water molecules is in progress and the results will be published in the future (Ślusarz et al., unpublished results).

V1aR–dDAVP and OTR–dDAVP Complexes

In both complexes, the residues equivalent to those in V2R also interact with the ligand. Therefore, the interactions with the highly conserved Gln residues occur, confirming their possible role in the mechanism of dDAVP binding. The most important specific interactions appear to be two analogous salt bridges, involving the D-Arg^{8} guanidinium and two carboxyls of either conserved $E^{1.35}$ (54 and 42 in V1aR and OTR, respectively) or nonconserved $D^{2.65}$(112,100) (see Figure 2C and D). This interaction is obviously absent in the V2R–dDAVP complexes, where the equivalent position occupies the positively charged $K^{2.65}100$. Accordingly, it has been demonstrated that the presence of $K^{2.65}100$ in V2R is adverse for dDAVP binding in the human V2 receptor, whereas the presence of aspartate at this position assists the binding of the dDAVP.[95] However, it has not affirmed whether the latter interact directly or indirectly with an agonist.[95] Similarly, as in the V2R–dDAVP complexes, the dislocation of the highly conserved arginyl (46 and 34 in V1aR and OTR, respectively) occurs, thus supporting our hypothesis that it might be involved in the receptor activation as described above. Similarly, as in the V2R–dDAVP complexes, any strong aromatic π–π interactions between receptor and ligand do not appear, except an insignificant interaction $F^{6.51}307$–Phe^{3} in the V1aR–dDAVP complex; only several hydrophobic or aromatic–hydrophobic interactions can be observed.

The V1aR and OTR residues identified as interacting with the $Gq/11_{\alpha}$(347–359) C-terminal segment are given in Table III. In general, the location of Gq/11α C-termini in both V1aR–dDAVP and OTR–dDAVP complexes has not been retained during MD. In the final complexes, both $Gq/11_{\alpha}$ peptides are partially displaced from the V1aR and OTR cavities toward the IL1 and intracellular side. This is probably a result of lack of some crucial stabilizing interactions at the receptor–$Gq/11_{\alpha}$(347–359) interface. The important interactions with two highly conserved motifs DRY/C (in V1aR and OTR, respectively) and NPxxY occur, however they are not as strong as in the V2R–dDAVP complexes. Similarly, the highly conserved $Gq/11_{\alpha}$ L353 and $L358^{42}$ only weakly interact with the receptor. The interactions with IL1 K(82,70) as well as $R^{6.32}$(288,272) appear in the V1aR and OTR, which have not been observed in V2R (see Table III). It is conceivable that all of the interactions observed in the V1aR–dDAVP and OTR–dDAVP complexes have been formed during the simulations (docking, CSA, energy minimization, and MD) and result simply from the ligand optimal fitting inside the binding

cavity, past the recognition step that actually implicates the binding of dDAVP to V1aR and OTR with a small affinity. This consequently results in inappropriate arrangement of other receptor residues and makes impossible their high affinity interaction with the G protein, allowing its partial dislocation from the receptor cavities.

Eventually, as in the V2R–dDAVP complexes, the internal water molecules in the ligand and Gq/11_{α}(347–359) vicinity can be observed in V1aR and OTR. They are accumulated within the receptor–ligand contact surfaces, interacting with polar, long-chain residues and in general are similar to V2R–dDAVP complexes, contributing to the stabilization of the receptor–ligand–G protein complexes.

Comparison of Modeling Results to Available Experimental Data

In the absence of experimentally determined 3D structures for vasopressin and oxytocin receptors, receptor models used in this study were constructed on the template of activated RD complexed with Gt_{α} C-terminal peptide.[45,46,96] Although it is agreed that RD makes a good structural template for other family A members,[3,9–13] using activated RD as a template for modeling other GPCR activated states is problematic and requires a validation for any specific case. Initially, the predicted receptor models were refined computationally by energy minimization followed by CSA to reduce the steric clashes.[46] However, the obtained models may be validated based on available experimental data for vasopressin/oxytocin receptor subfamily. Therefore, MD simulation (which efficiently samples conformational space) of agonist-bound receptor models was conducted and 12 complexes with endogenous hormones, vasopressin and oxytocin (six complexes per each ligand), were investigated.[46,47] The majority of receptor amino acid residues proposed as interacting with the ligands were previously identified as important for binding in experimental studies [46,47 and references therein]; the remaining receptor–ligand contacts provide guidelines for future experimental site-directed mutagenesis. Since, these two earlier studies[46,47] provided a partial refinement of the receptor structures, the same receptor models were consequently used to study the receptor–dDAVP interactions. In this investigation, the receptor–ligand complexes were generated by AutoDock.[54] Exclusively, in one V2R–dDAVP complex a D-Arg^8–D103 salt bridge was manually formed based on experimental evidence on the D103 relevance for dDAVP binding.[38] All remaining receptor–ligand interactions were formed during the simulation (docking, CSA, and energy minimization) and refined during 1-ns unconstrained MD. Comparing our modeling results with the available site-directed mutagenesis data for vasopressin and oxytocin receptors, the ligand-binding properties of several mutants are found to be in good agreement with the receptor–ligand complexes obtained in this study. These experimental data provide very useful information to validate our receptor models[64,68–70,73,92,95,97–105] (references assigned to specific residues are shown in Table II). As one may see in Table II, a majority of receptor–ligand contacts that occur in complexes obtained in this study were previously found to be involved in ligand binding for vasopressin/oxytocin receptor subfamily. For instance, a sigficant reduction in AVP affinity toward rat V1aR, reported for the $Q^{2.57}$A, $Q^{2.61}$A, $Q^{3.32}$A, and $Q^{6.55}$A mutants,[64] can be explained by their polar, direct interactions with the ligand observed in our models (see Figure 2, Table II, and above text). $Q^{4.60}$A mutant showed considerable impairment of AVP binding toward rat V1aR.[64] In V1aR and OTR, $Q^{4.60}$ directly interacts with the dDAVP, whereas in V2R there is the water-mediated interaction (see above text and Figures 2 and 9). The intricate network of hydrogen bonds is formed within the $K^{3.29}$116, $Q^{4.60}$174, $Q^{4.66}$180, $Q^{6.55}$291, Tyr^2 of dDAVP and water molecules (see Figure 9C), hence the disruption of this dense network of interaction may result in critical rearrangement of binding cavity and loss of ligand high-affinity binding. $Q^{2.61}$ is found to be in strong, polar interaction with the dDAVP D-Arg^8 side chain. Both $Q^{2.61}$A and $Q^{4.60}$A mutants demonstrated a substantial reduction in affinity to AVP,[64] thus suggesting that they are especially important determinants of AVP binding. Accordingly, in our model, $Q^{2.61}$ and $Q^{4.60}$ are located one helical turn closer to the extracellular side than $Q^{2.57}$, $Q^{3.32}$, and $Q^{6.55}$ (suggested as less important for AVP binding[64]); therefore, these two residues may be in addition involved in ligand recognition among vasopressin and oxytocin receptors. The moderate changes in AVP–V1aR affinity[64] resulting from $Q^{2.57}$A, $Q^{3.32}$A, and $Q^{6.55}$A mutations are also in agreement with our results. These residues, located somewhat deeper inside the binding cavity, form the hydrogen bonds with crucial dDAVP residues: Tyr^2 and Asn^5/Gln^4 (see Table II, Figure 2, and text above). In general, in the obtained models, all highly conserved Gln residues interact with the following ligand residues: Tyr^2, D-Arg^8, Asn^5/Gln^4. It is noticeable that residues at these amino acid positions are commonly known as especially important for agonistic activity among vasopressin/oxytocin receptor subfamily.[17,106–111]

Two other highly conserved residues, which have been previously proposed as critical for agonist binding toward vasopressin and oxytocin receptors are also involved in dDAVP binding in our models. Accordingly, it has been found in site-directed mutagenesis that the mutation of highly conserved N-terminal R (32, 46, and 34 in V2R, V1aR, and OTR, respectively) results in strong impairment of ligand binding.[68,69] This is in agreement with our models, where this conserved arginyl forms a hydrogen bond with the C-terminal carboxamide of dDAVP as described above (see also Figure 2). More recently it has been demonstrated that the highly conserved $E^{1.35}$ also plays an analogous role[70] and, in agreement with this finding, in our model this residue interacts via hydrogen bond with the C-terminal carboxamide (see Figure 2 and above text).

Detailed experimental data for human V2R also support validation of our receptor models, e.g., human V2R mutations involving the following residues: $L^{1.39}$44, $V^{2.53}$88, $W^{2.64}$99, EL2 R181, $I^{5.42}$209, $A^{6.58}$294, and $S^{7.43}$315 have been previously found as responsible for NDI by impairing AVP binding[65,73,92,97,98,105] and, accordingly all of these residues directly interact with dDAVP in our models (see Table II). Two other V2R residues identified in our study as interacing with dDAVP ($M^{3.36}$123, $S^{3.40}$127) also have been recognized as being responsible for NDI, but it is still undetermined whether they affect ligand binding.[112,113]

The obtained receptor–ligand models provide the information on receptor–ligand interactions at the molecular level that are sufficient to be validated by available experimental data. Moreover, the obtained models also generate hypotheses regarding the molecular details of GPCR function, i.e., receptor activation, G protein coupling, or internal water molecules role. These hypotheses might be next tested by experiments whose results, in turn, would be used to modify and refine molecular models.

CONCLUSION

The docking of dDAVP to neurohypophyseal hormone receptors and subsequent 1-ns MD simulation of complexes allowed us to propose a model of receptor–dDAVP interactions, involving both highly conserved and nonconserved receptor residues. A large part of the V2R–dDAVP interactions and those previously proposed for OT[46] and AVP[47] is common. Moreover, the majority of residues identified in this study have been previously determined in several experimental investigations to be involved in ligand binding for the neurohypophyseal hormone receptors subfamilies. The highly conserved residues have been proposed in this study as contributing to the network of interhelical interactions that, if broken, might initiate the conformational rearrangements during activation.

The nonconserved EL1 D103 recognized as crucial for V2R–dDAVP high affinity binding[38] has been proposed to be involved only in the ligand recognition. The receptor DRH/Y/C (in V2R, V1aR, and OTR, respectively) and NPxxY motifs, being the hallmarks for the family A GPCRs, have been identified to be involved in the G protein coupling. Two highly conserved Leu residues at the C-terminus of Gs_{α} protein appear to be mainly responsible for receptor binding. Eventually, the internal water molecules forming an intricate network of the hydrogen bonds inside the receptor cavity have been detected. These molecules appear to be involved in both dDAVP binding and in Gs_{α} coupling, contributing significantly to the stability of the whole system.

In summary, molecular models of receptor–ligand interactions might significantly facilitate rational design of new AVP analogs useful in several pathological conditions related to vasopressin V2 receptor. On the other hand, detailed knowledge on the V2R activation mechanism might assist in design of new ligands capable of activating the mutated V2R in NDI. Moreover, given the structural homology among Class A, these results might find an application in the design of drugs acting via other class A GPCRs.

This work is supported by The Polish Scientific Research Committee (KBN), Grant no. 3 T09A 116 28. Magdalena J. Ślusarz is supported by a L'Oréal–UNESCO "For Women in Science" Fellowship 2005 and European Social Fund (ESF) Scholarship no. ZPORR/2.22/II/2.6/ARP/U/2/05. The computational time in the Academic Computer Center in Gdansk CI TASK, Poland, and the Interdisciplinary Center for Mathematical Modeling (ICM) in Warsaw, Poland, is acknowledged.

REFERENCES

1. Bockaert, J.; Pin, J. P. EMBO J 1999, 18, 1723–1729.
2. Becker, O. M.; Shacham, S.; Marantz, Y.; Noiman, S. Curr Opin Drug Discov Dev 2003, 6, 353–361.
3. Ballesteros, J.; Palczewski, K. Curr Opin Drug Discov Dev 2001, 4, 561–574.
4. Hakak, Y.; Shrestha, D.; Goegel, M. C.; Behan, D. P.; Chalmers, D. T. FEBS Lett 2003, 550, 11–17.
5. Palczewski, K.; Kumasaka, T.; Hori, T.; Behnke, C. A.; Motoshima, H.; Fox, B. A.; Le Trong, I.;

Teller, D. C.; Okada, T.; Stenkamp, R. E.; Yamamoto, M.; Miyamoto, M. Science 2000, 289, 739–745.
6. Teller, D. C.; Okada, T.; Behnke, C. A.; Palczewski, K.; Stenkamp, R. E. Biochemistry 2001, 40, 7761–7772.
7. Okada, T.; Fujiyoshi, Y.; Silow, M.; Navarro, J.; Landau, E. M.; Shichida, Y. Proc Natl Acad Sci U S A 2002, 99, 5982–5987.
8. Okada, T.; Sugihara, M.; Bondar, A. N.; Elstner, M.; Entel, P.; Buss, V. J Mol Biol 2004, 342, 571–583.
9. Ballesteros, J. A.; Shi, L.; Javitch, J. A. Mol Pharmacol 2001, 60, 1–19.
10. Sakmar T. P. Curr Opin Cell Biol 2002, 14, 189–195.
11. Mirzadegan, T.; Benko, G.; Filipek, S.; Palczewski, K. Biochemistry 2003, 42, 2759–2767.
12. Archer, E.; Maigret, B.; Escrieut, C.; Pradayrol, L.; Fourmy, D. Trends Pharmacol Sci 2003, 24, 36–40.
13. Oliveira, L.; Hulsen, T.; Lutje Hulsik, D.; Paiva, A. C.; Vriend, G. FEBS Lett 2004, 564, 269–273.
14. Ślusarz, M. J.; Ślusarz, R.; Kaümierkiewicz, R.; Trojnar, J.; Wiśniewski, K.; Ciarkowski, J. Protein Pept Lett 2003, 10, 295–302.
15. Ślusarz, M. J.; Ślusarz, R.; Meadows, R.; Trojnar, J.; Ciarkowski, J. QSAR Comb Sci 2004, 23, 536–545.
16. Ślusarz, M. J.; Gieswsl. ldoñ, A.; Ślusarz, R.; Meadows, R.; Trojnar, J.; Ciarkowski, J. QSAR Comb Sci 2005, 24, 603–610.
17. Barberis, C.; Mouillac, B.; Durroux, T. J Endocrinol 1998, 156, 223–229.
18. Zingg, H. H.; Baillieres Clin Endocrinol Metab 1996, 10, 75–96.
19. Thibonnier, M.; Berti-Mattera, L. N.; Dulin, N.; Conarty, D. M.; Mattera, R. Prog Brain Res 1998, 119, 147–161.
20. Birnbaumer, M.; Seibold, A.; Gilbert, S.; Ishido, M.; Barberis, C.; Antaramian, A.; Brabet, P.; Rosenthal, W. Nature 1992, 357, 333–335.
21. Birnbaumer, M. Arch Med Res 1999, 30, 465–474.
22. Thibonnier, M.; Auzan, C.; Madhun, Z.; Wilkins, P.; Berti-Mattera, L.; Clauser, E. J Biol Chem 1994, 269, 3304–3310.
23. Sugimoto, T.; Saito, M.; Mochizuki, S.; Watanabe, Y.; Hashimoto, S.; Kawashima, H. J Biol Chem 1994, 269, 27088–27092.
24. Kimura, T.; Tanizawa, O.; Mori, K.; Brownstein, M. J.; Okayama, H. Nature 1992, 356, 526–529.
25. Gimpl, G.; Fahrenholz, F. Physiol Rev 2001, 81, 629–683.
26. Barberis, C.; Tribollet, E. Crit Rev Neurobiol 1996, 10, 119–154.
27. Hunyady, L.; Vauquelin, G.; Vanderheyden, P. TIPS 2003, 24, 81–86.
28. Lebl, M.; Jošt, K.; Brtník, F. In Handbook of Neurohypophysial Hormone Analogs, Vol. 1, Part 2; CRC Press: Boca Raton, FL, 1987; pp 127–267.
29. Robertson, G. L.; Berl, T. Pathophysiology of Water Metabolism: The Kidney,6th ed.; Philadelphia: W.B. Saunders, 2000; pp 866–924.
30. Richardson, D. W.; Robinson, A.G. Ann Intern Med 1985, 103, 228–239.
31. Zaoral, M. Int J Pept Protein Res 1985, 25, 561–574.
32. Fukuda, I.; Hizuka, N.; Takano, K. Endocr J 2003, 50, 437–443.
33. Schulman, S. L.; Stokes, A.; Salzman, P. M. J Urol 2001, 166, 2427–2431.
34. White, B.; Lawler, P.; Riddell, A.; Nitu-Whalley, I. C.; Hermans, C.; Lee, C. A.; Brown, S. A. Br J Haematol 2004, 126, 100–104.
35. Mannucci, P. M. N Engl J Med 2004, 351, 683–694.
36. Lethagen, S.; Egervall, K.; Berntorp, E.; Bengtsson, B. Haemophilia 1995, 1, 97–102.
37. Hruby, V. J.; Chow, M-S. Annu Rev Pharmacol Toxicol 1990, 30, 501–534.
38. Ufer, E.; Postina, R.; Gorbulev, V.; Fahrenholz, F. FEBS Lett 1995, 362, 19–23.
39. Hubbell, W. L.; Altenbach, C.; Hubbell, C. M.; Khorana, H. G. Adv Protein Chem 2003, 63, 243–290.
40. Farrens, D. L.; Altenbach, C.; Yang, K.; Hubbell, W. L.; Khorana, H. G. Science 1996, 274, 768–770.
41. Koenig, B. W. Chembiochem 2002, 3, 975–980.
42. Kisselev, O. G.; Kao, J.; Ponder, J. W.; Fann, Y. C.; Gautam, N.; Marshall, G. R. Proc Natl Acad Sci U S A 1998, 95, 4270–4275.
43. Janz, J. M.; Farrens, D. L. J Biol Chem 2004, 279, 29767–29773.
44. Koenig, B. W.; Kontaxis, G.; Mitchell, D. C.; Louis, J. M.; Litman, B. J.; Bax, A. J Mol Biol 2002, 322, 441–461.
45. Ślusarz, R.; Ciarkowski, J. Acta Biochim Pol 2004, 51, 129–136.
46. Ślusarz, M. J.; Ślusarz, R.; Ciarkowski, J. J Pept Sci 2006, 12, 171–179.
47. Ślusarz, M. J.; Gieldoń, A.; Ślusarz, R.; Ciarkowski, J. J Pept Sci 2006, 12, 180–189.
48. Case, D. A.; Pearlman, D. A., Caldwell, J. W., Cheatham, T. E.; Wang, J.; Ross, W. S.; Simmerling, C. L.; Darden, T. A.; Merz, K. M.; Stanton, R. V.; Cheng, A.; Vincent, J. J.; Crowley, M.; Tsui, V.; Gohlke, H.; Radmer, R.; Duan, Y.; Pitera, J.; Massova, I.; Seibel, G. L.; Singh, U. C.; Weiner, P.; Kollman, P. A. Amber 7. 2002, University of California, San Francisco.
49. Cieplak, P.; Cornell, W. D.; Bayly, C.; Kollman, P. A. J Comp Chem 1995, 16, 1357–1377.
50. Schmidt, M. W.; Baldridge, K. K.; Boatz, J. A.; Elbert, S. T.; Gordon, M. S.; Jensen, J. H.; Koseki, S.; Matsunaga, N.; Nguyen, K. A.; Su, S.; Windus, T. L.; Dupuis, M.; Montgomery, J. A. J Comput Chem 1993, 14, 1347–1363.
51. Langs, D. A.; Smith, G. D.; Stezowski, J. J.; Hughes, R. E. Science 1986, 232, 1240–1242.
52. Sybyl 6.8, Tripos Inc. 1699 South Hanley Rd., St. Louis, MO 63144, USA.
53. Kirkpatrick, S.; Gelatt, C. D., Jr.; Vecchi, M. P. Science 1983, 220, 671–680.
54. Morris, G. M.; Goodsell, D. S.; Halliday, R. S.; Huey, R.; Hart, W. E.; Belew, R. K.; Olson, A. J. J Comput Chem 1998, 19, 1639–1662.
55. Solis, F.J.; Wets, J.B. Math Oper Res 1981, 6, 19–30.

56. Goodsell, D. S.; Morris, G. M.; Olson, A. J. J Mol Recognit 1996, 9, 1–5.
57. Ślusarz, R.; Ślusarz, M. J.; Kaümierkiewicz, R.; Lammek, B. QSAR 2003, 22, 865–872.
58. Murzyn, K.; Róg, T.; Jezierski, G.; Takaoka, Y.; Pasenkiewicz-Gierula, M. Biophys J 2001, 81, 170–183.
59. Pasenkiewicz-Gierula, M. Murzyn, K.; Róg, T.; Czaplewski, C. Acta Biochim Polon 2000, 47, 601–611.
60. Essmann, U. L.; Perera, M. L.; Berkowitz, T.; Darden, T.; Lee, H.; Pedersen, L. G. J Chem Phys 1995, 103, 8577–8593.
61. Jorgensen, W.L.; Tirado-Rives, J. J Am Chem Soc 1988, 110, 1657–1666.
62. Guex, N.; Peitsch, M. C. Electrophoresis 1997, 18, 2714–2723.
63. Ballesteros, J. A.; Weinstein, H. Methods Neurosci 1995, 25, 366–428.
64. Mouillac, B.; Chini, B.; Balestre, M. N.; Elands, J.; Trumpp, K. S.; Hoflack, J.; Hibert, M.; Jard, S.; Barberis, C. J Biol Chem 1995, 270, 25771–25777.
65. Morello, J. P.; Salahpour, A.; Petaja-Repo, U. E.; Laperriere, A.; Lonergan, M.; Arthus, M. F.; Nabi, I. R.; Bichet, D. G.; Bouvier, M. Biochemistry 2001, 40, 6766–6775.
66. Strosberg, A. D.; Camoin, L.; Blin, N.; Maigret, B. Drug Design Discov 1993, 9, 199–211.
67. Kim, J-M.; Altenbach, C.; Kono, M.; Oprian, D. D.; Hubbell, W. L.; Khorana, H. G. Proc Natl Acad Sci U S A 2004, 101, 12508–12513.
68. Hawtin, S. R.; Wesley, V. J.; Parslow, R. A.,Simms, J.; Miles, A.; McEwan, K.; Wheatley, M. Mol Endocrinol 2002, 16, 600–609.
69. Wheatley, M.; Hawtinm S. R.; Wesley, V. J.; Howard, H. C.; Simms, J.; Miles, A.; McEwan, K.; Parslow, R. A.; Biochem Soc Trans 2003, 31, 35–39.
70. Hawtin, S. R.; Wesley, V. J.; Simms, J.; Argent, C. C. H.; Latif, K.; Wheatley, M. Mol Endocrinol 2005, 11, 2871–2881.
71. Manning, M.; Olma, A.; Klis, W.; Kolodziejczyk, A.; Nawrocka, E.; Misicka, A.; Seto, J.; Sawyer, W. H.; Nature 1984, 308, 5960–5961.
72. Chruścinska, E.; Derdowska, I.; Kozlowski, H.; Lammek, B.; Luczkowski, M.; Oldziej, S.; Świątek-Kozlowska, J. New J Chem 2003, 27, 251–256.
73. Albertazzi, E.; Zanchetta, D.; Barbier, P.; Faranda, S.; Frattini, A.; Vezzoni, P.; Procaccio, M.; Bettinelli, A.; Guzzi, F.; Parenti, M.; Chini, B. J Am Soc Nephrol 2000, 11, 1033–1043.
74. Colson, A-O.; Perlman, J. H.; Jinsi-Parimoo, A.; Nussenzveig, D. R.; Osman, R.; Gershengorn, M. C. Mol Pharmacol 1998, 54, 968–978.
75. Rosenthal, W.; Antaramian, A.; Gilbert, S.; Birnbaumer, M. J Biol Chem 1993, 268, 13030–13033.
76. Fanelli, F.; Barbier, P.; Zanchetta, D.; De Benedetti, P. G.; Chini, B. Mol Pharmacol 1999, 56, 214–225.
77. Scheer, A.; Fanelli, F.; Costa, T.; De Benedetti, P. G.; Cotecchia, S. EMBO J 1996, 15, 3566–3578.
78. Ballesteros, J.; Kitanovic, S.; Guarnieri, F.; Davies, P.; Fromme, B. J.; Konvicka, K.; Chi, L.; Millar, R. P.; Davidson, J. S.; Weinstein, H.; Sealfon, S. C. J Biol Chem 1998, 273, 10445–10453.
79. Zhu, S. Z.; Wang, S. Z.; Hu, J.R.; Elfakahany, E. E.; Mol Pharmacol 1994, 45, 517–523.
80. Acharya, S.; Karnik, S. A. J Biol Chem 1996, 271, 25406–25411.
81. Rasmussen, S. G. F.; Jensen, A. D.; Liapakis, G.; Ghanouni, P.; Javitch, J. A.; Gether, U. Mol Pharmacol 1999, 56, 175–184.
82. Alewijnse, A. E.; Timmerman, H.; Jacobs, E. H.; Smit, M. J.; Roovers, E.; Cotecchia, S.; Leurs, R.; Mol Pharmacol 2000, 57, 890–898.
83. Rosenkilde, M. M.; Kledal, T. M.; Schwartz, T. W. Mol Pharmacol 2005, 68, 11–19.
84. Hawtin, S. R.; Mol Pharmacol 2005, 68, 1172–1182.
85. Barak, L. S.; Menard, L.; Ferguson, S. S.; Colapietro, A. M.; Caron, M. G. Biochemistry 1995, 34, 15407–15414.
86. Hunyady, L.; Bor, M.; Baukal, A. J.; Balla, T.; Catt, K. J. J Biol Chem 1995, 270, 16602–16609.
87. Galés, C.; Kowalski-Chauvel, A.; Dufour, M-N.; Seva, C.; Moroder, L.; Pradayrol, L.; Vaysse, N.; Fourmy, D.; Silvente-Poirot, S. J Biol Chem 2000, 275, 17321–17327.
88. Urizar, E.; Claeysen, S.; Deupí, X.; Govaerts, C.; Costagliola, S.; Vassart, G.; Pardo, L. J Biol Chem 2005, 280, 17135–17141.
89. Garcia, P. D.; Onrust, R.; Bell, S. M.; Sakmar, T. P.; Bourne, H. R. EMBO J 1995, 14, 4460–4469.
90. Osawa, S.; Weiss, E. R. J Biol Chem 1995, 270, 31052–31058.
91. Martin, E. L.; Rens-Domiano, S.; Schatz, P. J.; Hamm, H. E. J Biol Chem 1996, 271, 361–366.
92. Ala, Y.; Morin, D.; Mouillac, B.; Sabatier, N.; Vargas, R.; Cotte, N.; Déchaux, M.; Antignac, C.; Arthus, M-F.; Lonergan, M.; Turner, M.; Balestre, M-N.; Alonso, G.; Hibert, M.; Barberis, C.; Hendy, G. N.; Bichet, D.; Jard, S. J Am Soc Nephrol 1998, 9, 1861–1872.
93. Luecke, H.; Schobert, B.; Richter, H.-T.; Cartailler, J. P.; Lanyi, J. K. J Mol Biol 1999, 291, 899–911.
94. Shibata, M.; Kandori, H. Biochemistry 2005, 44, 7406–7413.
95. Cotte, N.; Balestre, M-N.; Phalipou, S.; Hibert, M.; Manning, M.; Barberis, C.; Mouillac, B. J Biol Chem 1998, 273, 29462–29468.
96. Ślusarz, R.; Ślusarz, M. J.; Lammek, B.; Ciarkowski, J. QSAR Comb Sci 2005, DOI: 10.1002/qsar. 200430920.
97. Oksche, A.; Schülein, R.; Rutz, C.; Liebenhoff, U.; Dickson, J.; Müller, H.; Birnbaumer M.; Rosenthal, W. Mol Pharmacol 1996, 50, 820–828.
98. Knoers, N. V.; van den Ouweland A. M.; Verdijk, M.; Monnens, L. A.; van Oost, B. A. Kidney Int 1994, 46, 170–176.
99. Kojro, E.; Postina, R.; Gilbert, S.; Bender, F.; Krause, G.; Fahrenholz, F. Eur J Biochem 1999, 266, 538–548.

100. Cotte, N.; Balestre, M-N.; Aumelas, A.; Mahé, E.; Phalipou, S.; Morin, D.; Hibert, M.; Manning, M.; Durroux, T.; Barberis, C.; Mouillac, B. Eur J Biochem 2000, 267, 4253–4263.
101. Breton, C.; Chellil, H.; Kabbaj-Benmansour, M.; Carnazzi, E.; Seyer, R.; Phalipou, S.; Morin, D.; Durroux, T.; Zingg, H.; Barberis, C.; Mouillac, B. J Biol Chem 2001, 276, 26931–26941.
102. Tahtaoui, C.; Balestre, M-N.; Klotz, P.; Rognan, D.; Barberis, C.; Mouillac, B.; Hibert, M. J Biol Chem 2003, 278, 40010–40019.
103. Postina, R.; Ufer, E.; Pfeiffer, R.; Knoers, N. V.; Fahrenholz, F. Mol Cell Endocrinol 2000, 164, 31–39.
104. Acharjee, S.; Do-Rego, J-L.; Oh, D-Y.; Ahn, R. S.; Choe, H.; Vaudry, H.; Kim, K.; Seong, J. Y.; Kwon, H. B. J Biol Chem 2004, 279, 54445–54453.
105. Pan, Y.; Wilson, P.; Gitschier, J. J Biol Chem 1994, 269, 31933–31937.
106. Manning, M.; Sawyer, W. H. In Vasopressin; Schrier, R. W, Ed.; Raven Press: New York, 1985; pp 131–144.
107. Walter, R. Fed Proc Am Soc Exp Biol 1977, 36, 1872–1878.
108. Chan, W. Y.; Wo, N. C.; Cheng, L. L.; Manning, M. J Pharmacol Exp Ther 1996, 277, 999–1003.
109. Sawyer, W. H.; Acosta, M.; Balaspiri, L.; Judd, J.; Manning, M. Endocrinology 1974, 94, 1106–1115.
110. Gillessen, D.; du Vigneaud, V. J Biol Chem 1967, 242, 4806–4812.
111. Postina, R.; Kojro, E.; Fahrenholz F. J Biol Chem 1996, 271, 31593–31601.
112. Arthus, M. F.; Lonergan, M.; Crumley, M. J.; Naumova, A. K.; Morin, D.; De Marco, L. A.; Kaplan, B. S.; Robertson, G. L.; Sasaki, S.; Morgan, K.; Bichet, D. G.; Fujiwara, T. M. J Am Soc Nephrol 2000, 11, 1044–1054.
113. Morello, J. P.; Bichet, D. G.; Annu Rev Physiol 2001, 63, 607–630.
114. Manning, M.; Balaspiri, L.; Moehring, J.; Haldar, J.; Sawyer, W. H. J Med Chem 1976, 19, 842–845.
115. Bernstein, H. J.; TIBS 2000, 25, 453–455.
116. Koradi, R.; Billeter, M.; Wüthrich, K. J Mol Graphics 1996, 14, 51–55.
117. Corpet, F. Nucleic Acids Res 1998, 16, 10881–10890.

Reviewing Editor: J. McCammon